Clim Dyn (2018) 50:991–1006
DOI 10.1007/s00382-017-3656-3

Impacts of the Pacific Meridional Mode on Landfalling North Atlantic tropical cyclones

Wei Zhang[1] · Gabriele Villarini[1] · Gabriel A. Vecchi[2,3] · Hiroyuki Murakami[2,3]

Received: 19 September 2016 / Accepted: 21 March 2017 / Published online: 6 April 2017

Abstract This study examines the impacts of the Pacific Meridional Mode (PMM) on North Atlantic tropical cyclones (TCs) making landfall along the coastal US, Caribbean Islands and Mexico, and provides insights on the underlying physical mechanisms using observations and model simulations. There is a statistically significant time-lagged association between spring PMM and the August–October US and Caribbean landfalling TCs. Specifically, the positive (negative) spring PMM events tend to be followed by fewer (more) TCs affecting the coastal US (especially over the Gulf of Mexico and Florida) and the Caribbean Islands. This lagged association is mainly caused by the lagged impacts of PMM on the El Niño Southern Oscillation (ENSO), and the subsequent impacts of ENSO on TC frequency and landfalls. Positive (negative) PMM events are largely followed by El Niño (La Niña) events, which lead to less (more) TC geneses close to the US coast (i.e., the Gulf of Mexico and the Caribbean Sea); this also leads to easterly (westerly) steering flow in the vicinity of the US and Caribbean coast, which is unfavorable (favorable) to TC landfall across the Gulf of Mexico, Florida and Caribbean Islands. Perturbation simulations with the state-of-the-art Geophysical Fluid Dynamics Laboratory Forecast-oriented Low Ocean Resolution Version of CM2.5 (FLOR) support the linkage between PMM and TC landfall activity. The time-lagged impacts of spring PMM on TC landfalling activity results in a new predictor to forecast seasonal TC landfall activity along the US (especially over the Gulf of Mexico and Florida) and Caribbean coastal regions.

Keywords Landfall · Tropical Cyclones · Pacific Meridional Mode

✉ Wei Zhang
wei-zhang-3@uiowa.edu

[1] IIHR-Hydroscience and Engineering, The University of Iowa, Iowa City, IA, USA

[2] Geophysical Fluid Dynamics Laboratory, National Oceanic and Atmospheric Administration, Princeton, NJ, USA

[3] Atmospheric and Oceanic Sciences Program, Princeton University, Princeton, NJ, USA

1 Introduction

North Atlantic tropical cyclones (TCs) are one of the costliest and most catastrophic natural hazards affecting the US (e.g., Pielke Jr et al. 2008; Smith and Katz 2013). TCs cause severe damages to the coastal and inland regions during or after landfall (e.g., Pielke Jr and Landsea 1999; Pielke Jr et al. 2008), with significant impacts due to strong winds, heavy rainfall, flooding, and storm surge. Despite the significant societal and economic impacts associated with these storms, the prediction of TC landfall statistics is still a very challenging problem (e.g., Marks and Shay 1998; Saunders and Lea 2005; Elsner and Jagger 2006; Vecchi and Villarini 2014; Vecchi et al. 2014; Murakami et al. 2016). It is therefore of crucial importance to better understand what controls the frequency and variability of landfalling TCs in terms of climate processes, which in turn can lay the foundation for better predictions.

In general, the US TC landfall activity tends to be suppressed (enhanced) during El Niño (La Niña) events (e.g., Bove et al. 1998; Pielke Jr and Landsea 1999; Elsner 2003; Tang and Neelin 2004; Elsner and Jagger 2006; Smith et al. 2007) because of the modulation of the vertical wind shear and steering flow in the North Atlantic (e.g., Bove et al. 1998; Klotzbach 2011; Staehling and Truchelut 2016). After the identification of the central Pacific El Niño/Warm

Pool El Niño (CP El Niño; e.g., Ashok et al. 2007; Weng et al. 2007; Kug et al. 2009), several studies have been devoted to the analysis of whether, how and to what extent CP El Niño modulates TC landfall (Kim et al. 2010; Lee et al. 2010; Larson et al. 2012; Wang et al. 2014; Patricola et al. 2016). In addition to ENSO, there are other climate modes that have been found to be related to the frequency and tracking of US landfalling TCs. For instance, the Atlantic warm pool, which is a large body of warm water covering the Gulf of Mexico, the Caribbean Sea, and the western tropical North Atlantic, has been found to modulate TC landfall rate by changing both genesis locations and steering flow (Wang and Lee 2007; Wang et al. 2008, 2011). In particular, large (small) sizes of the Atlantic warm pool tend to produce steering flow unfavorable (favorable) to TC landfall along the US coast; this then leads to a smaller (larger) number of TCs in the main development region (MDR) than climatology in the presence of a large (small) Atlantic warm pool (Wang and Lee 2007; Wang et al. 2008, 2011). Moreover, the Atlantic Multidecadal Oscillation (AMO) and the Atlantic Meridional Mode can also influence the modulation of ENSO on TC landfall (Vimont and Kossin 2007; Klotzbach 2011; Patricola et al. 2014), while the North Atlantic Oscillation (NAO) has been found to affect TC landfall by changing the steering flow and subtropical ridge (e.g., Xie et al. 2005; Kossin et al. 2010; Villarini et al. 2011).

In addition to these climate modes, recent work has linked ENSO and the Pacific Meridional Mode (PMM), which is defined as the first Maximum Covariance Analysis (MCA) of sea surface temperature (SST) and the zonal and meridional components of the 10 m wind field (Chiang and Vimont 2004). PMM acts effectively as a conduit through which the extra-tropical atmosphere influences ENSO (e.g., Anderson 2003, 2004; Chang et al. 2007; Boschat et al. 2013). The North Pacific Oscillation (NPO) is a north–south seesaw in sea level pressure over the North Pacific (Walker and Bliss 1932), exerting strong impacts of El Niño/La Niña (e.g., Vimont et al. 2001, 2003; Ding et al. 2015). For example, the NPO/Victoria mode can affect the onset of El Niño/La Niña in which PMM acts as a bridge by the seasonal footprinting mechanism (SFM) and the wind-evaporation-SST feedback (Vimont et al. 2001, 2003; Chiang and Vimont 2004; Ding et al. 2015), indicating that PMM is closely linked with the development of ENSO (Chang et al. 2007; Zhang et al. 2009a, b; Kim et al. 2012; Pegion and Alexander 2013; Larson and Kirtman 2014; Di Lorenzo et al. 2015; Ding et al. 2015; Lin et al. 2015). During winter (year−1), the midlatitude atmospheric variability (e.g., NPO) exerts an SST "footprint" (anomaly) to the ocean surface by changing the net surface heat flux (Vimont et al. 2001, 2003). The SST anomaly can persist into the spring and summer season (year0) in subtropics (i.e., PMM) and force changes in atmospheric circulation associated with zonal wind stress anomalies in the tropical equatorial region. These equatorial zonal wind stress anomalies (caused by the SFM) are considered as key source of stochastic atmospheric forcing for tropical ENSO variability in the following (year+1) winter (Vimont et al. 2001, 2003). Positive (negative) values of PMM that peaks in spring are largely followed by El Niño (La Niña) events (Chang et al. 2007; Zhang et al. 2009a, b; Larson and Kirtman 2014). Around 46% of the variability of ENSO in the mature phase can be explained by the PMM index during the previous January–May (Chang et al. 2007). In terms of TC activity, for instance, PMM strongly modulates the occurrence of the Eastern Pacific hurricanes (Murakami et al. 2017) and typhoons in the western North Pacific by mediating vertical wind shear and this association is verified in both observations and long control experiments using a coupled climate model (Zhang et al. 2016, 2017).

The association between PMM and ENSO, and that between ENSO and landfalling TCs suggests that PMM may influence the frequency of North Atlantic TCs making landfall along the coastlines. The goal of this study is, therefore, to examine the role played by PMM via ENSO in controlling the frequency and tracking of landfalling TCs. By advancing our understanding of the physical processes controlling landfalling activity, we will provide basic information that can lead to the improved seasonal predictions of these storms.

This paper is organized as follows. Section 2 presents the data and methodology, while Sect. 3 discusses the results based on observations and simulations. Section 4 includes the discussion and summarizes the main conclusions.

2 Data and methodology

The information about North Atlantic TCs is based on latitude, longitude and time of occurrence of TCs. TC data are obtained from the National Oceanic and Atmospheric Administration's (NOAA) National Hurricane Center's best-track database (HURDAT2; Landsea and Franklin 2013) available for the period 1851–2015. We use the Met Office Hadley Center (HadISST, version 1.1; Rayner et al. 2003) as reference SST data, while the atmospheric variables are obtained from the National Centers for Environmental Prediction (NCEP)/National Center for Atmospheric Research (NCAR) reanalysis project (NCEP-NCAR; Kalnay et al. 1996).

We divide the US coastline facing the Gulf of Mexico and the Atlantic Ocean into four main regions (Fig. 1): Southwest (Gulf of Mexico), Florida, Southeast and Northeast. We also analyze North Atlantic TCs making landfall over Caribbean islands and Mexico (Fig. 1). We consider as

Fig. 1 The six regions used to define TC landfall including Southwest (Gulf of Mexico, *green*), Florida (*orange*), Southeast (*purple*), Northeast (*blue*), Caribbean Islands (*red*) and Mexico (*dark blue*)

a landfalling TC affecting any of these regions if the center of circulation of the storm is within 300 km from the coastline (sensitivity analyses with buffers from 100 to 500 km showed similar results). Moreover, we focus only on storms that occurred during the August–October months (ASO) as this is the peak of North Atlantic TC season.

Steering flow is used to analyze the environmental flow that leads to the changes in TC tracks, and is defined as the deep-layer mean wind fields from 850 to 200 hPa levels (e.g., Chan and Gray 1982; Velden et al. 1992).

The PMM index is calculated following the methodology described in Chiang and Vimont (2004). In calculating it, the seasonal cycle and the linear trend of SST and 10-m wind field are first removed by applying a 3-month running mean to the data, and then subtracting the linear fit to the cold tongue index (CTI) (Deser and Wallace 1987) from the spatial grids to remove correlations with El Niño (Chiang and Vimont 2004). The CTI is defined as the SST anomalies averaged over 6°S–6°N, 180°W–90°W minus the global mean SST. The 10 years with the largest positive/negative MAM PMM values are listed in Table 1.

Figure 2 depicts the PMM pattern represented by the regression of SST and surface wind fields onto the PMM index in both observations and climate simulations with the Geophysical Fluid Dynamics Laboratory (GFDL) Forecast-oriented Low Ocean Resolution Version of CM2.5 or FLOR. The PMM pattern in the positive phase is characterized by a warming (cooling) in the northwestern (southeastern) part of the subtropical and tropical eastern Pacific, coupled with surface winds (Fig. 2). Overall, FLOR realistically captures the

Table 1 List of the 10 years with the strongest positive and negative MAM PMM values during the 1948–2015 period

PMM phases	Years
Positive PMM	1954, 1959, 1966, 1967, 1968, 1980, 1986, 1994, 1995, 2015
Negative PMM	1975, 1976, 1983, 1998, 1999, 2000, 2001, 2008, 2011, 2012

fundamental structure of PMM in the observations (Fig. 2), as also reported in Zhang et al. (2016, 2017).

We define Niño3.4 index as the SST anomalies over the region 5°N–5°S, 120°–170°W, Niño3 index as the SST anomalies over the region 5°N–5°S and 150°W–90°W, and Niño4 index as the SST anomalies over the region 5°N–5°S, 160°E–150°W. SST anomalies are defined with respect to the 1970–2000 base period.

We use the genesis potential index (GPI; Emanuel and Nolan 2004) to examine the potential of TC genesis during the peak seasons when PMM in the previous spring is strongly positive or negative. GPI is defined as:

$$\mathrm{GPI} = \left|10^5\eta\right|^{\frac{3}{2}}\left(\frac{\mathcal{H}}{50}\right)^3\left(\frac{\mathrm{V_{pot}}}{70}\right)^3\left(1+0.1\mathrm{V_{shear}}\right)^{-2} \quad (1)$$

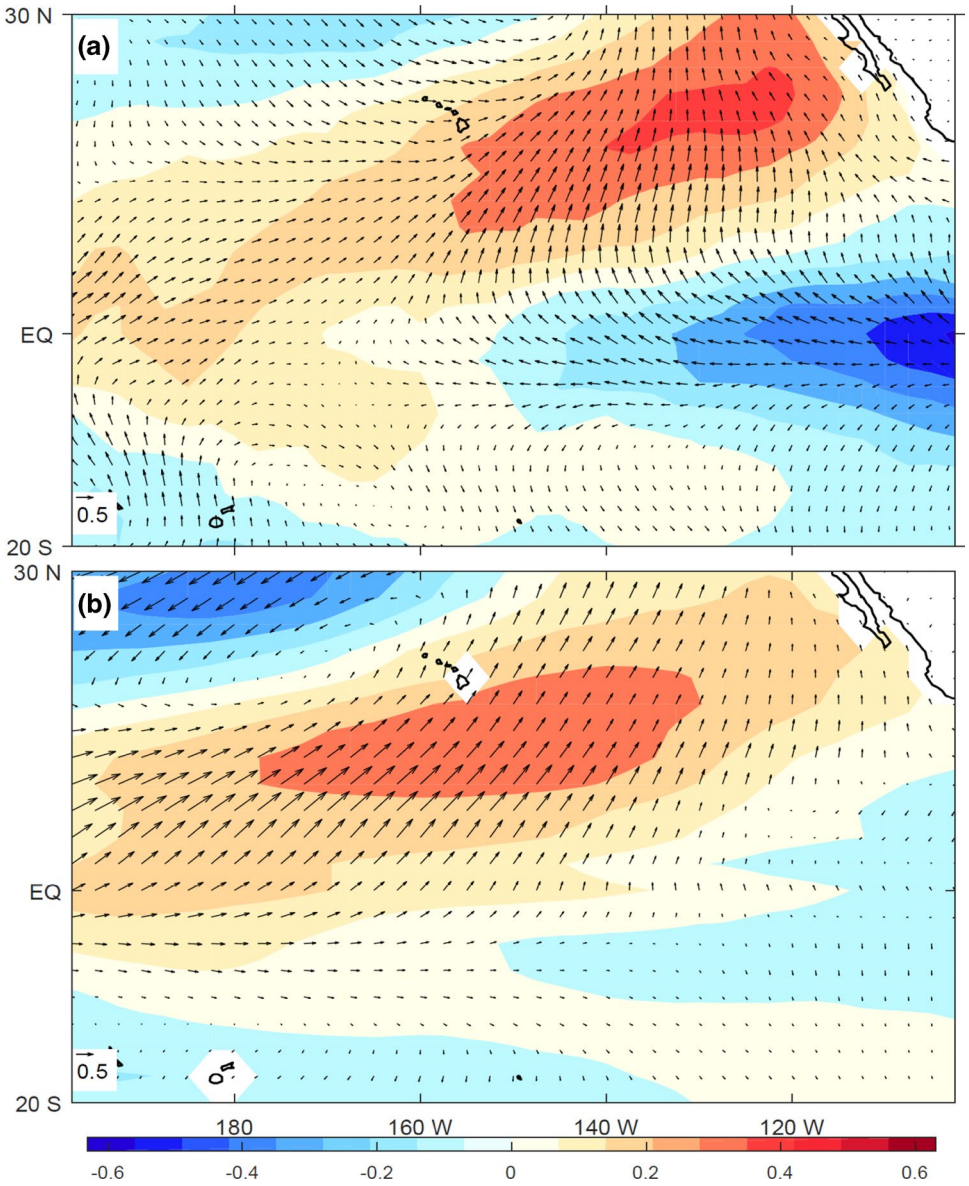

Fig. 2 The regression of SST (*shading* unit: °C) and 10 m wind fields (*vector* unit: ms^{-1}) onto the PMM index in **a** observations and **b** FLOR control experiments

where η is is absolute vorticity at 850 hPa level, $\mathcal{H}$ is the relative humidity at 600 hPa level (unit: percent), v_{pot} is the potential intensity (unit: ms^{-1}), and V_{shear} is the vertical wind shear between 850 and 200 hPa levels. GPI involves thermodynamic and dynamic variables that are important for TC genesis. GPI has been widely used to analyze genesis potential in observations and climate models across different basins.

We complement the results from observational and reanalysis datasets using a newly-developed high-resolution coupled climate model (FLOR) for perturbation experiments (Vecchi et al. 2014). The capability of FLOR in representing the frequency, intensity, track, seasonality and genesis of global TCs and in forecasting global TC activity has been described in previous studies (e.g., Vecchi et al. 2014; Murakami et al. 2016; Zhang et al. 2016, 2017).The atmosphere and land components of this model are from the GFDL CM2.5 with a spatial resolution of 50 km × 50 km (Delworth et al. 2012) while its ocean and sea ice components are similar to those in the CM2.1 with a spatial resolution of 1° × 1° (Delworth et al. 2006). We use the flux-adjusted version of FLOR (FLOR-FA) (Vecchi et al. 2014). More details about FLOR/FLOR-FA are discussed in Vecchi et al. (2014) and references therein. We use a tracker to obtain TC tracks from FLOR simulations (Zhang et al. 2016). TC track and genesis densities in observations and FLOR simulations are obtained by binning TCs into 5° × 5° box with Boxcar spatial filter (with size 3 × 3) to smooth local variations. GPI is also smoothed by the Boxcar spatial filter (with size 3 × 3).

We perform a set of perturbation experiments to isolate the role of the PMM in forcing the changes in TC

activity and tracking. In the control run (CTRL), SST is restored to a repeating annual cycle of the SST climatology in the 1860 control run with a 10-day restoring timescale (*tau*). The restoring of SST in the model to the observed estimates is represented by:

$$\frac{\mathrm{dSST}}{\mathrm{dt}} = \varsigma + \frac{\mathrm{SSTo} - \mathrm{SST}}{\mathrm{tau}} \quad (2)$$

A restoring tendency was applied to the SST tendency as computed in the coupled model (ς) over a restoring time scale *tau* [tau is the constant restoring time scale (e.g., 5-day or 10-day)]; dSST represents the change of SST and dt change of time. SSTo represents a space- and time-dependent array of the observed estimates of SST, while SST is the SST simulated by the model. The larger the *tau*, the more relaxed the coupling and the weaker the nudging/restoring of SST. A free run with a fully-coupled model has a *tau* of infinity while Atmospheric Model Intercomparison Project (AMIP) run has a *tau* of zero. The restoring time scale is set as 10-day because this allows the changes of simulated SST, which is different from AMIP runs in which SST is considered as boundary forcing and cannot be changed. In the perturbation experiment, we prescribe the sum of the annual cycle of SST and the temporally constant SST anomalies associated with the positive PMM patterns (denoted as PPMM) at the 10-day scale. We select the 10-day restoring time scale to permit atmosphere–ocean feedbacks including TC-ocean feedbacks and to prevent large-scale SST biases. After an initial 100-year spinup, both experiments are integrated for 60 years.

3 Results

The March–May averaged (MAM) PMM index has significant associations with the frequency of ASO TC landfall over the Gulf of Mexico, Florida, the entire US coast, the Caribbean Islands and Mexico (Table 2). The southern part of the US coast includes the Gulf of Mexico and Florida, which are subject to the largest number of landfalling TCs each year. The correlation coefficient between the MAM PMM index and the number of peak-season (ASO) TCs making landfall over the Gulf of Mexico and Florida for the 1948–2015 is −0.36, and significant at the 0.05 level. However, the correlation coefficients between the PMM index in JJA and ASO and TC landfall activity are much smaller compared to those computed with respect to the MAM PMM. The correlation coefficient between the MAM PMM index and the number of peak-season (ASO) TCs making landfall over the Caribbean Islands is −0.30 which is significant at the 0.05 level (Table 2). Moreover, we do not find a statistically significant correlation with the other regions. To substantiate the correlation coefficient, Table 3 shows the frequency of TCs making landfall over the regions during positive, negative and neutral PMM phases. The positive (negative) PMM phase includes the years with the MAM PMM index larger (smaller) than one (minus one) standard deviation, while the remaining years are considered as neutral years. In general, the frequencies of landfalling TCs during the positive PMM phase are lower than those during negative PMM phase, particularly when there are significant correlations between the frequency of landfalling TCs and the PMM index (e.g., Gulf, Florida, Gulf

Table 2 Correlation coefficients between PMM in March–May (MAM), June–August (JJA) and August–October (ASO) and the frequency of landfalling TCs over different coastal regions (1948–2015)

	Gulf	Florida	Gulf & Florida	Southeast	Northeast	US Coast	Caribbean	Mexico
PMM (MAM)	−0.26*	−0.35*	−0.36*	−0.20	−0.15	−0.32*	−0.30*	−0.21
PMM (JJA)	−0.06	−0.20	−0.15	−0.06	−0.04	−0.12	−0.23	−0.04
PMM (ASO)	−0.13	−0.22	−0.20	−0.10	−0.007	−0.15	−0.27*	−0.08

The symbol "*" represents the correlation coefficients which are significant at the 0.05 significance level. "Gulf and Florida" represents TCs that made landfall over the Gulf of Mexico and Florida combined

Table 3 Average frequencies of landfalling TCs over different coastal regions during positive, negative and neutral PMM phases (1948–2015)

	Gulf	Florida	Gulf and Florida	Southeast	Northeast	US Coast	Caribbean	Mexico
PMM (positive)	1.1	1.5	2.0	1.5	1.4	2.6	2.2	1.6
PMM (negative)	2.2	3.2	4.0	2.3	2.0	4.6	3.6	2.1
PMM (neutral)	1.9	2.4	3.1	2.4	1.9	4.0	3.0	1.7

The positive (negative) PMM phase includes the years with the MAM PMM index larger (smaller) than one (minus one) standard deviation, while the remaining years are considered as neutral years

and Florida and Caribbean Islands) (Tables 2, 3). For example, there are four TCs making landfall over Gulf and Florida on average during the negative PMM phase, which is twice the average frequency during the positive PMM phase (Table 3).

The time series of the MAM PMM index and the ASO TC landfall frequency are shown in Fig. 3. Overall, when the PMM index in spring is positive, there are fewer peak-season TCs making landfall, while the opposite is true for the negative PMM values. For example, the spring PMM index is negative in 1953, 1969, 1971, 1987, 1998, 1999, 2002, 2008 while the peak-season TC landfall over the Gulf of Mexico and Florida is quite active (Fig. 3a). Similar results are shown for the entire US coast and Caribbean Islands (Fig. 3, panels b, c). This suggests that there is a marked time-lagged association between PMM and the frequency of landfalling TCs over the Gulf of Mexico, Florida, the US coast and Caribbean islands. The 10 years with strong positive PMM index have less TC landfalls than those with strong negative positive PMM index (Fig. 3; Table 1).

Figure 4 illustrates the histogram and fitted Gaussian distribution of MAM PMM indices in the 20 years with the highest and the lowest TC landfall frequency, respectively. Higher/lower landfall frequencies over the Gulf of Mexico, Florida, Gulf of Mexico and Florida combined, the entire US coast, Mexico and the Caribbean Islands are associated with lower/higher values of the PMM index, supported by the clear shift in the histogram and fitted distributions (Fig. 4). This further supports the lagged linkage between spring PMM and peak-season TC landfall.

Figure 5 depicts the TC density anomalies during the 10 years with the largest absolute values of the MAM PMM (Table 1). TC density anomalies are characterized by a dipole when the MAM PMM phase is positive (Fig. 5a); there is a large positive area of TC density in the eastern North Atlantic while there is a high negative area in the western North Atlantic, Gulf of Mexico, Caribbean region,

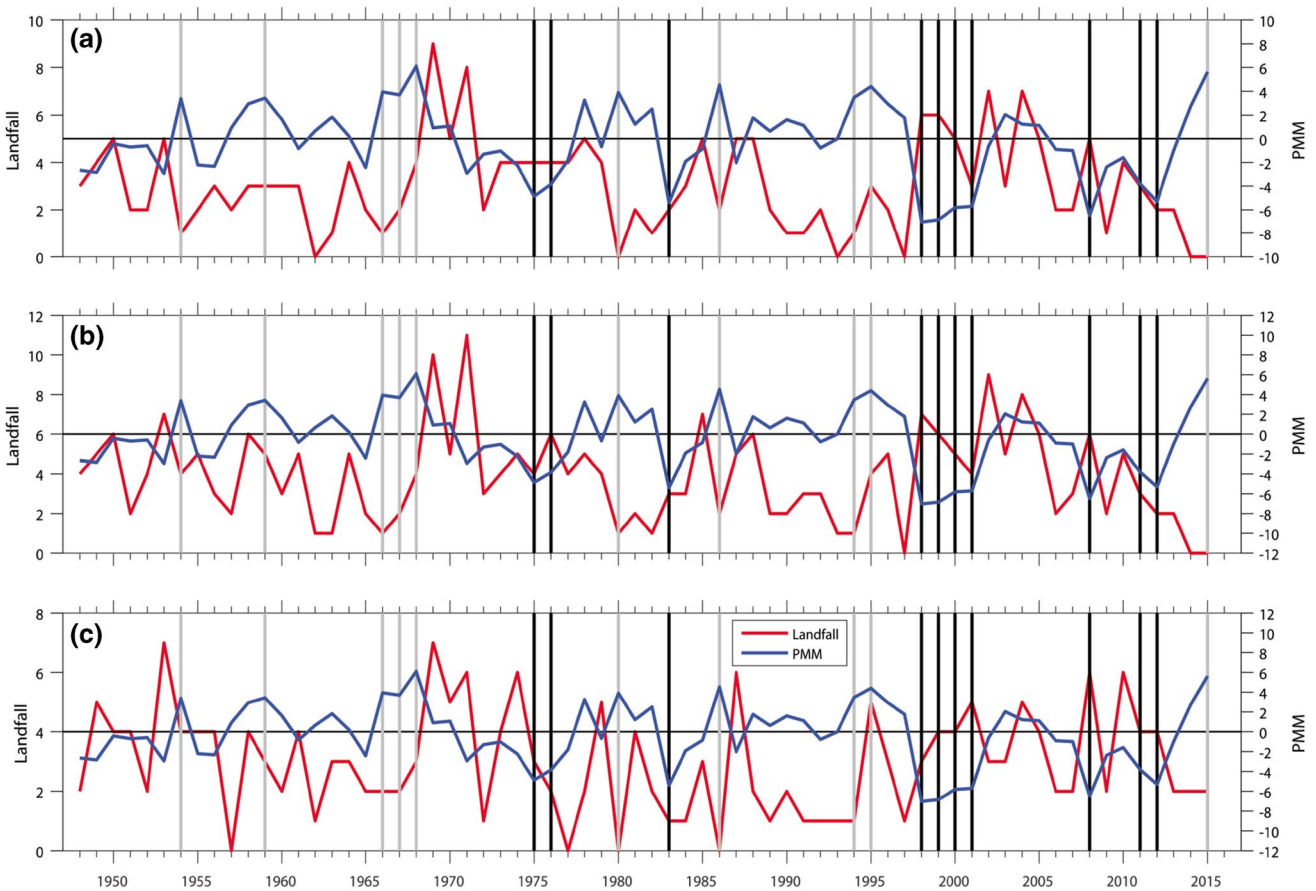

Fig. 3 Time series of the MAM PMM index and the number of landfalling TCs during the August–October period. **a** The storms making landfall along the Gulf of Mexico and Florida (correlation coefficient of −0.36), **b** the number of storms making landfall along the US coastline (correlation coefficient of −0.32), and **c** the number of storms making landfall along the Caribbean islands (correlation coefficient of −0.30). The *grey* and *black vertical lines* represent 10 years (Table 1) with strong positive and negative PMM values in MAM, respectively

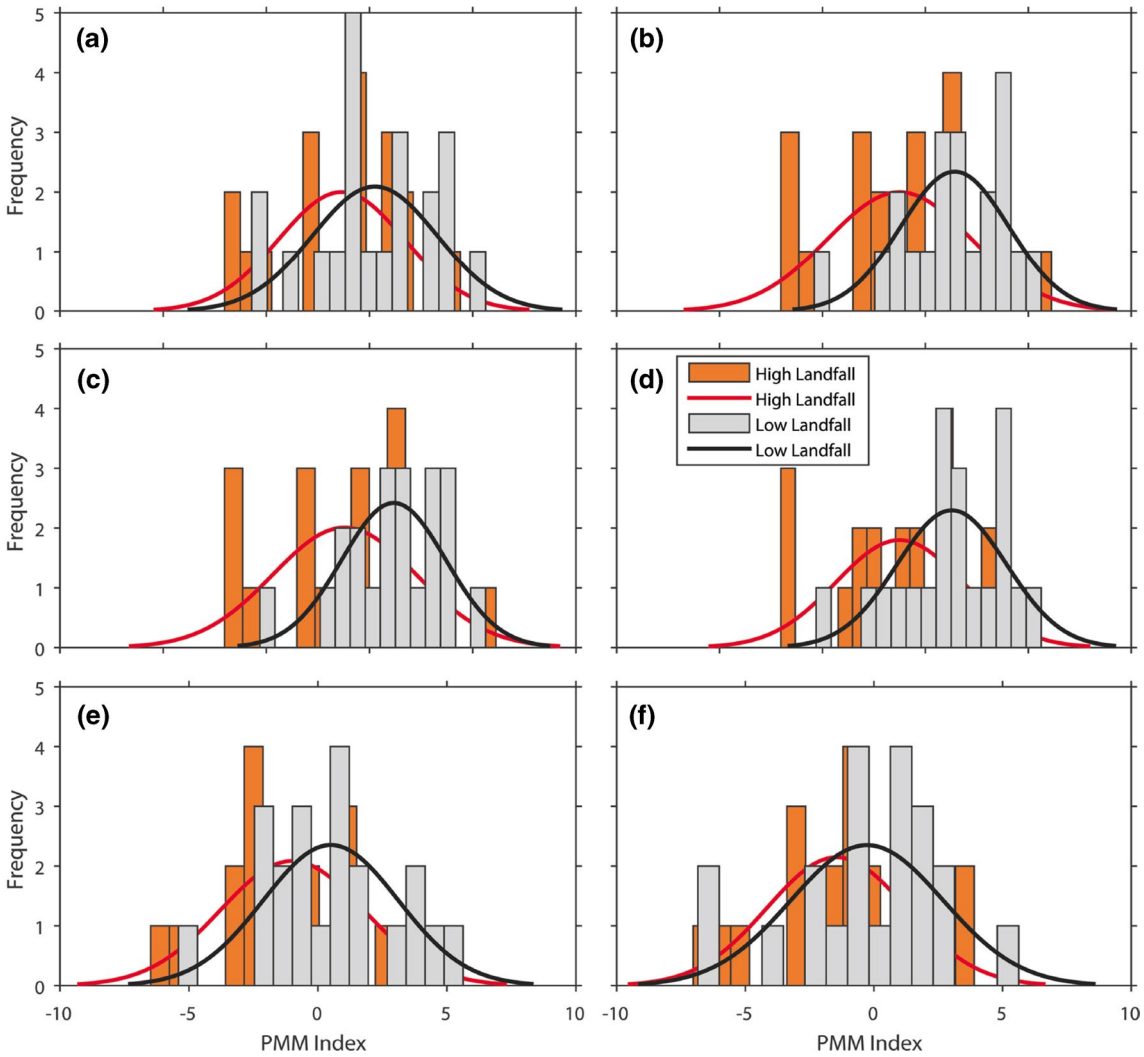

Fig. 4 Histogram and fitted Gaussian distribution of the MAM PMM indices when the frequency of landfalling TCs during ASO is the highest (*red*) or the lowest (*black*) over **a** Gulf, **b** Florida, **c** Gulf of Mexico and Florida, **d** the entire US coast, **e** Caribbean islands and **f** Mexico

and the US coast when MAM PMM is positive. This suggests fewer TC landfalls over the US coast (especially over the Gulf of Mexico and Florida) and the Caribbean Islands (Fig. 5a). When MAM PMM is negative, the TC density anomalies are largely opposite to those discussed for the positive MAM PMM (Fig. 5b). These findings are consistent with the negative correlation between MAM PMM and ASO TC landfall (Fig. 3; Table 2). During the positive (negative) MAM PMM, there is largely suppressed (enhanced) TC activity in the North Atlantic basin and along the US coast and Caribbean Islands (Fig. 5).

Because TC density anomalies are strongly influenced by changes in TC genesis and steering flow (e.g., Wang et al. 2011; Colbert and Soden 2012), we analyze changes in these two quantities to interpret the changes in TC density with respect to the PMM phases. TC genesis anomalies are characterized by negative anomalies in the Gulf of Mexico and western North Atlantic and positive anomalies in the eastern North Pacific when MAM PMM is positive (Fig. 6a). This is in good agreement with the negative TC density anomalies along the southern US coast (Fig. 5a). When MAM PMM is negative, TC genesis density features positive anomalies in part of the Gulf of Mexico. The genesis anomalies are generally positive compared with those during the positive spring PMM, albeit the anomalies are located in a small region in the North Atlantic (Fig. 6b). TC genesis anomalies in the North Atlantic have a larger magnitude during the positive MAM PMM than those during the negative MAM PMM, in particular in the Gulf of Mexico and Caribbean Islands (Fig. 6). Therefore, TC genesis density anomalies during the peak season are mainly consistent with TC

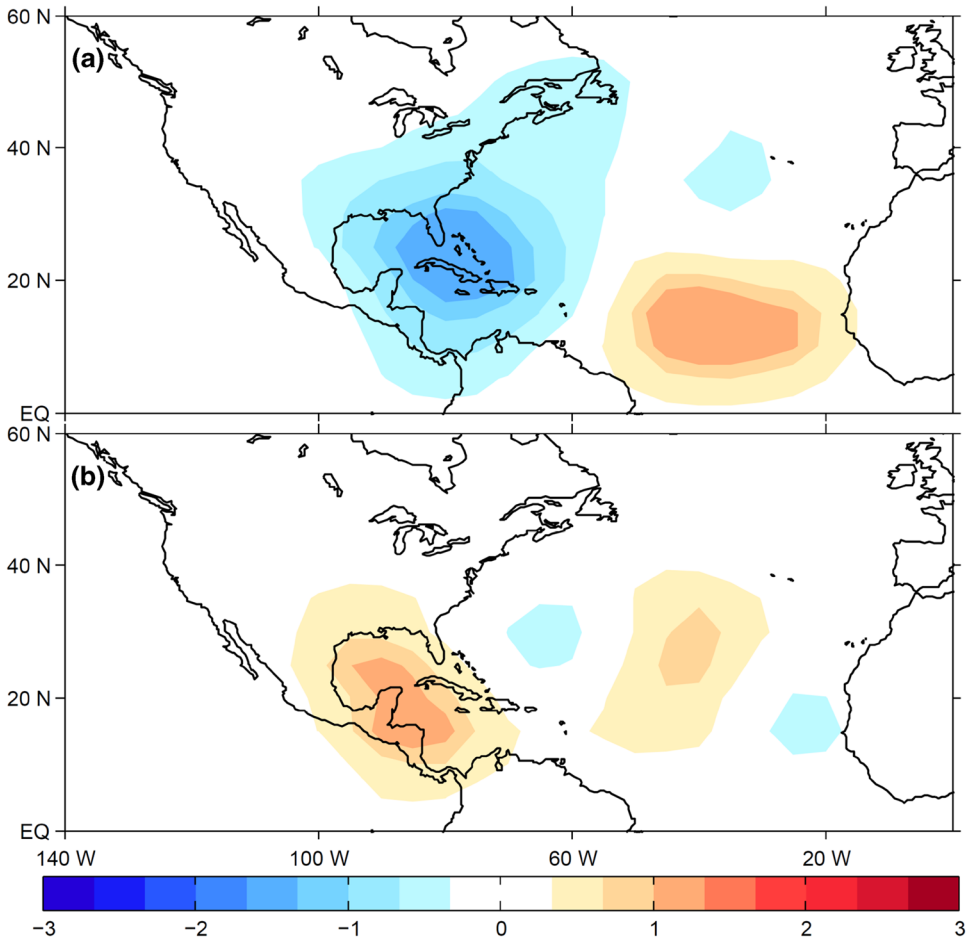

Fig. 5 ASO TC track density anomalies (*shading* unit: occurrences/season) when MAM PMM is **a** positive and **b** negative. Hurricane track density is calculated by binning hurricane tracks into 5° × 5° grid boxes. The base period for climatology is 1948–2015

density anomalies during the positive or negative MAM PMM phases (Figs. 5, 6).

GPI is also consistent with the genesis density anomalies during the different PMM phases. For example, the GPI anomalies are largely positive (negative) in the Gulf of Mexico, Caribbean and western North Atlantic, consistent with the positive (negative) TC genesis anomalies during the negative (positive) MAM PMM (Fig. 7). There are strong positive GPI anomalies north of 25°N, which may be related to the positive SST anomalies in those regions associated with La Niña in the tropical Pacific (Fig. 7b). Climatologically, few TCs form north of 25°N in the North Atlantic. Therefore, the positive GPI anomalies north of 25°N during the negative PMM phase do not exert strong impacts on TC genesis (Fig. 6b). On the other hand, there are differences with respect to GPI and TC genesis in the tropical eastern Atlantic, where stronger GPI anomalies correspond to weaker TC genesis anomalies during the negative PMM phase compared to the positive one (Fig. 7).

4 Physical mechanisms

4.1 Time-lagged modulation

The results so far have highlighted the significant time-lagged association between PMM and TC landfall. Here we focus on the physical mechanisms underlying this lagged association. A number of studies have documented that PMM is mostly followed by ENSO events (e.g., Chang et al. 2007; Zhang et al. 2009a, b; Larson and Kirtman 2014). We hypothesize that this lagged association is caused by the PMM-ENSO-TC linkage.

Figure 8 displays that the time series of MAM PMM, and Niño3, Niño3.4 and Niño4 indices averaged over ASO. The correlation coefficients between the PMM (wind) index in the spring and Niño4, Niño3, Niño3.4 in ASO have values of 0.50, 0.42, and 0.48, respectively; these results are statistically significant at the 0.05 level, and consistent with previous findings that PMM is largely followed by ENSO (e.g., Chang et al. 2007; Zhang et al. 2009a, b; Larson and Kirtman 2014). The correlation coefficients between

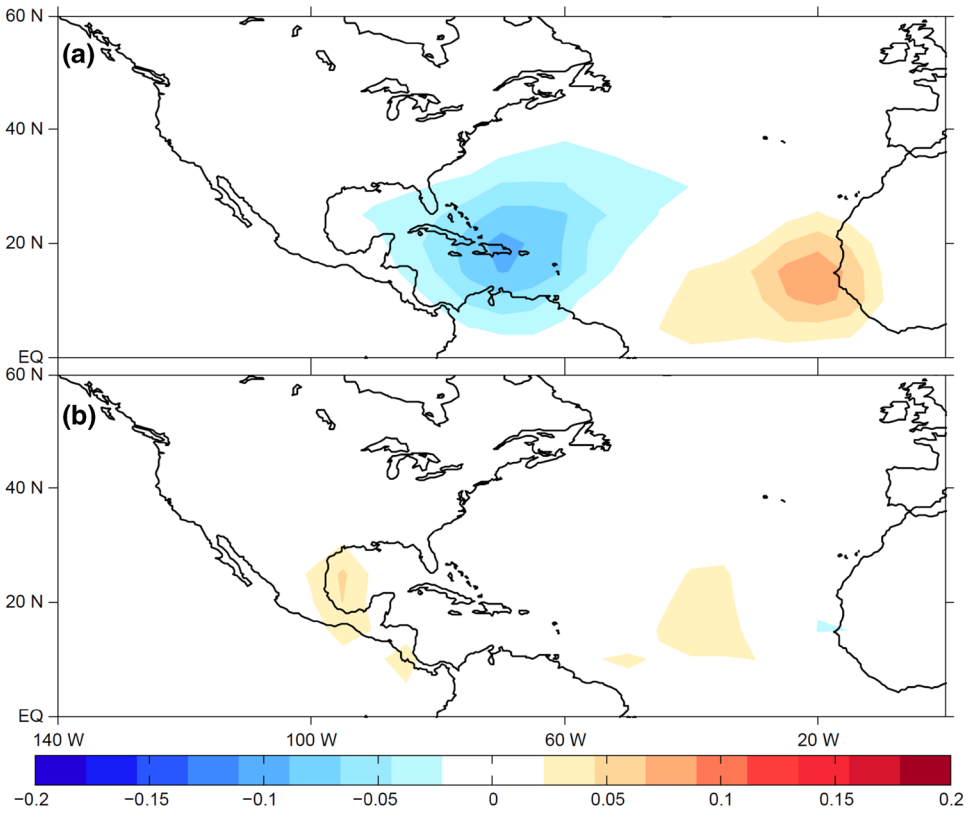

Fig. 6 ASO TC genesis density anomalies (*shading* unit: occurrences/season) when MAM PMM is **a** positive and **b** negative. TC genesis density is calculated by binning the storm tracks into 5° × 5° grid boxes. The base period for climatology is 1948–2015

the PMM (SST) index in the spring and Niño4, Niño3, Niño3.4 in ASO are similar to those obtained for the PMM (wind) index shown above. The correlation between PMM and Niño4 is higher than those between PMM and Niño3 and Niño3.4, indicating that the PMM may have a slightly higher chance to be followed by the central Pacific El Niño (El Niño Modoki) than by the eastern Pacific El Niño (e.g., Kim et al. 2012; Ding et al. 2015; Lin et al. 2015), at least based on the observations.

To further substantiate these statistical results, we select the 10 years with the strongest positive and the 10 years with the strongest negative MAM PMM (Table 1). We composite the SST and steering flow anomalies in MAM, JJA, ASO, and OND. During the positive MAM PMM, the typical PMM mode with positive (negative) SST anomalies in its northwestern (southeastern) part is very strong, while the steering flow in the Atlantic and US sector is negligible along or close to the US coast (Fig. 9a). During JJA, the strong positive SST anomalies in the northwestern part of the PMM pattern propagate southeastward towards the tropical Central Pacific. Accompanying this, there are strong northwesterly steering flow anomalies along the US coast (Fig. 9b). During ASO (i.e., peak TC season), the positive SST anomalies have moved further southeastward in the tropical central and eastern Pacific and the steering flow anomalies are stronger than in the previous months (Fig. 9c). Such steering flow pattern is detrimental to the TC landfall over the US coast: these results provide a mechanism to understand why PMM in the spring impacts TC landfalling activity in the US. However, the steering flow is not significant along the US, Mexican, and Caribbean coasts during ASO (Fig. 9). Finally, during OND, an El Niño-like pattern in the tropics develops (Fig. 9d).

The years characterized by a strongly negative MAM PMM present patterns that are largely the opposite of what described for the positive years. During the positive MAM PMM, there are warm (cool) SST anomalies in the southeastern (northwestern) portion of the tropical and subtropical eastern Pacific (Fig. 10a). There is also an anomalous easterly steering flow over the southeastern and northeastern part of the US coast, while there is westerly flow over Florida and the Caribbean regions (Fig. 10a). During JJA, the cooling moves equatorward, while the warming diminishes in the southeastern part, in contrast to what observed in MAM. The anomalous steering flow over Florida and the Caribbean changes from westerly to easterly (Fig. 10b). During ASO, the warming in the southeastern part almost disappears, while a La Niña-like pattern develops in the tropical central and eastern Pacific (Fig. 10c). Corresponding to this SST pattern, the anomalous easterly steering flow tends to steer TCs to make landfall over the coastal regions (Fig. 10c). It is noted that the steering flow is not statistically significant along the Caribbean coast. The propagation of SST warming from the subtropical eastern

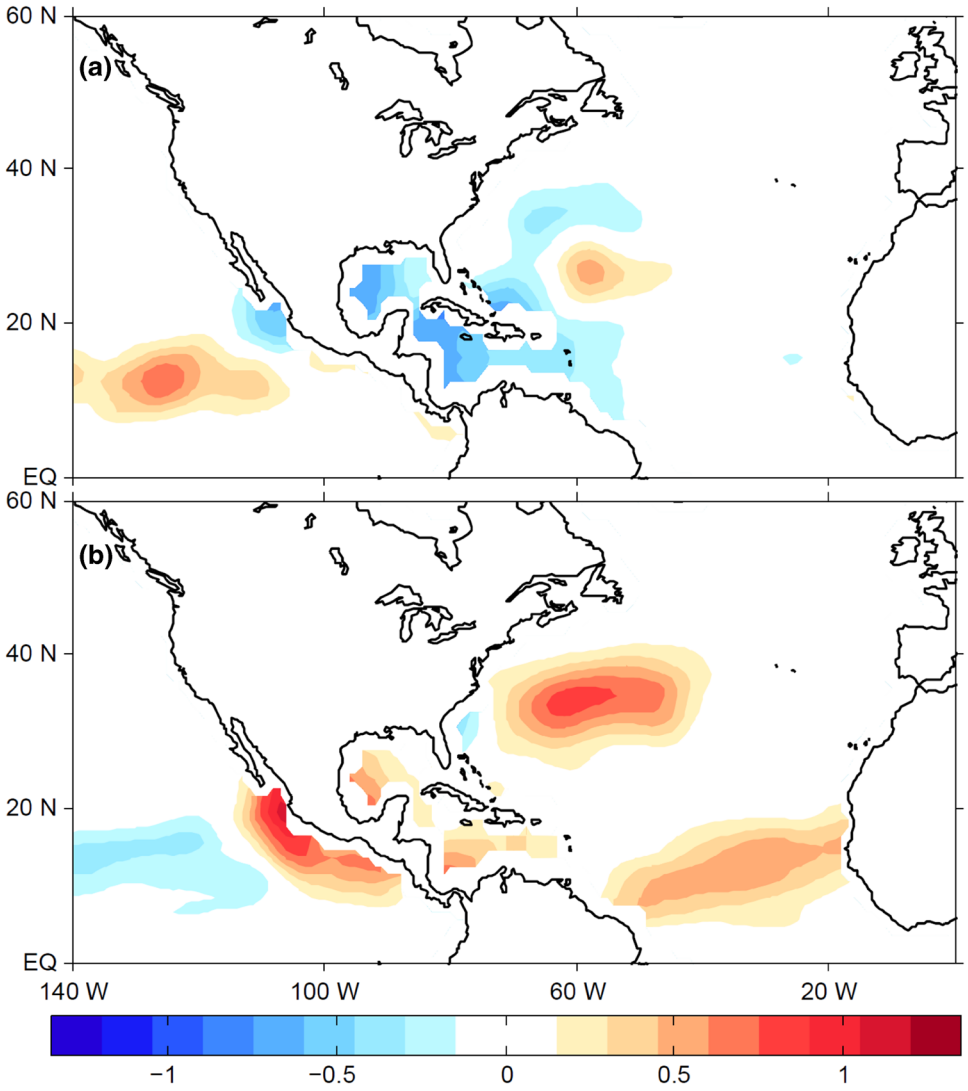

Fig. 7 ASO TC genesis potential index anomalies (*shading* unit: occurrences/season) when MAM PMM is **a** positive and **b** negative

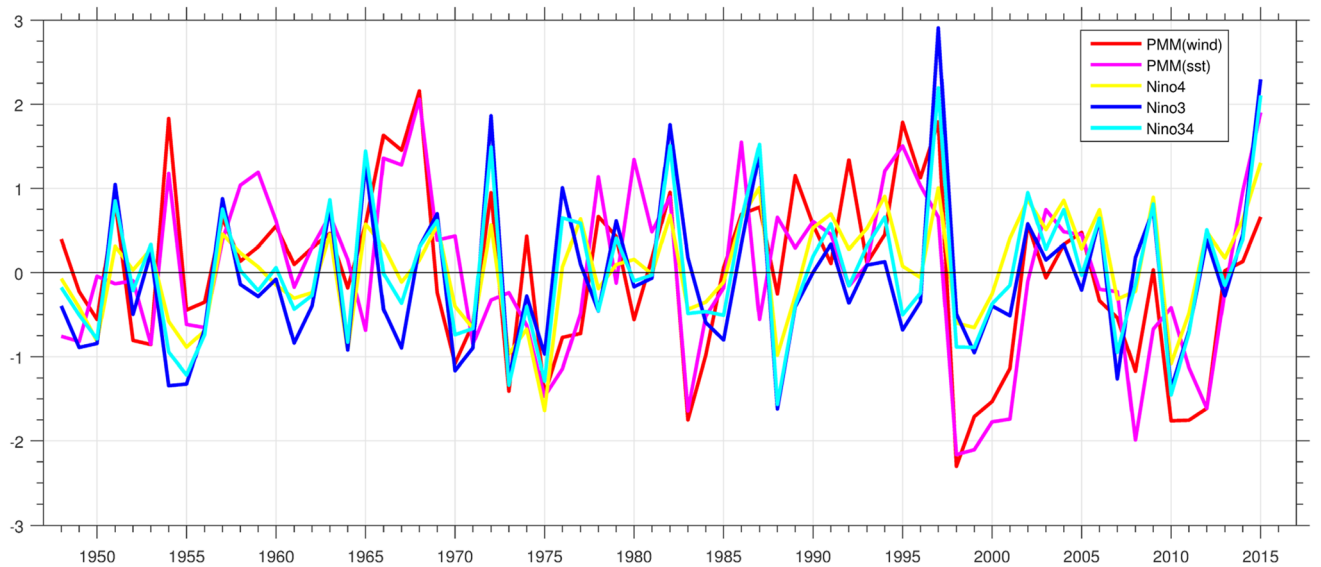

Fig. 8 Time series of PMM (wind and SST) in March–May (*red* and *magenta*, respectively), and Niño4 (*yellow*), Niño3 (*blue*), Niño3.4 (*cyan*) indices averaged over the August–October for the period 1948–2105. The PMM index (wind and SST) is normalized

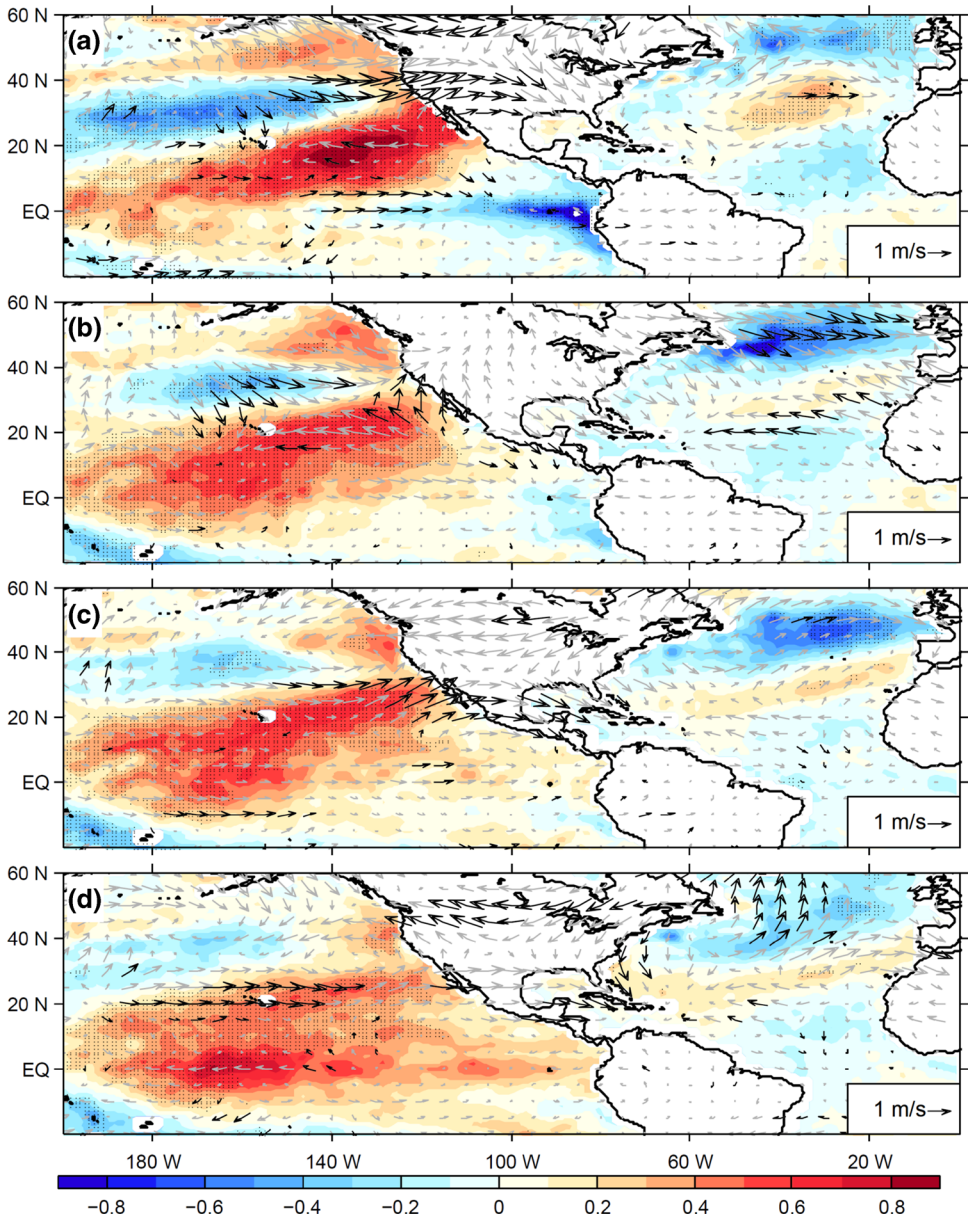

Fig. 9 Composite SST (*shading* unit: °C; see *color bar*) and steering flow (*wind vectors*) anomalies during MAM, JJA, ASO, and OND when the MAM PMM is in the positive phase. Stippled regions denote the places which are statistically significant at the 0.05 level. The black wind vectors are statistically significant at the 0.05 level

Pacific to the tropics is supported by the wind-evaporation-SST feedback associated with thermodynamic air–sea coupling (e.g., Xie and Philander 1994; Chang et al. 1997; Chiang and Bitz 2005) which have been widely used in analyses of this kind. During OND, the easterly steering flow anomalies become even stronger, while the La Niña-like SST anomalies prevail in the tropical central and eastern Pacific (Fig. 10d).

The impacts of ENSO on steering flow have been widely discussed in the literature (e.g., Camargo et al. 2007; Kossin et al. 2010; Colbert and Soden 2012; Wang et al. 2014; Li et al. 2015). A typical Matsuno-Gill-type (Matsuno 1966; Gill 1980) response of the atmosphere can be induced over the tropical Atlantic and there is a weakening of the North Atlantic Subtropical High causing anomalous cyclonic flow in the eastern mid-Atlantic during El Niño (La Niña) seasons, which is conductive to less (more) TC landfalls (e.g., Colbert and Soden 2012; Kossin et al. 2010; Li et al. 2015). ENSO events, especially those in the central Pacific, are strongly associated with the Pacific-North American Pattern (PNA) (e.g., Ashok et al. 2007; Weng et al. 2007, 2009), which may also bridge the influences of PMM on steering flow.

Therefore, the steering flow anomalies during the positive and negative PMM phases largely support the time-lagged relationship between MAM PMM and ASO TC landfall. However, the steering flow is not statistically significant in the Caribbean coast during negative PMM phase whereas it is largely not significant along the US, Caribbean and Mexican coast during positive PMM

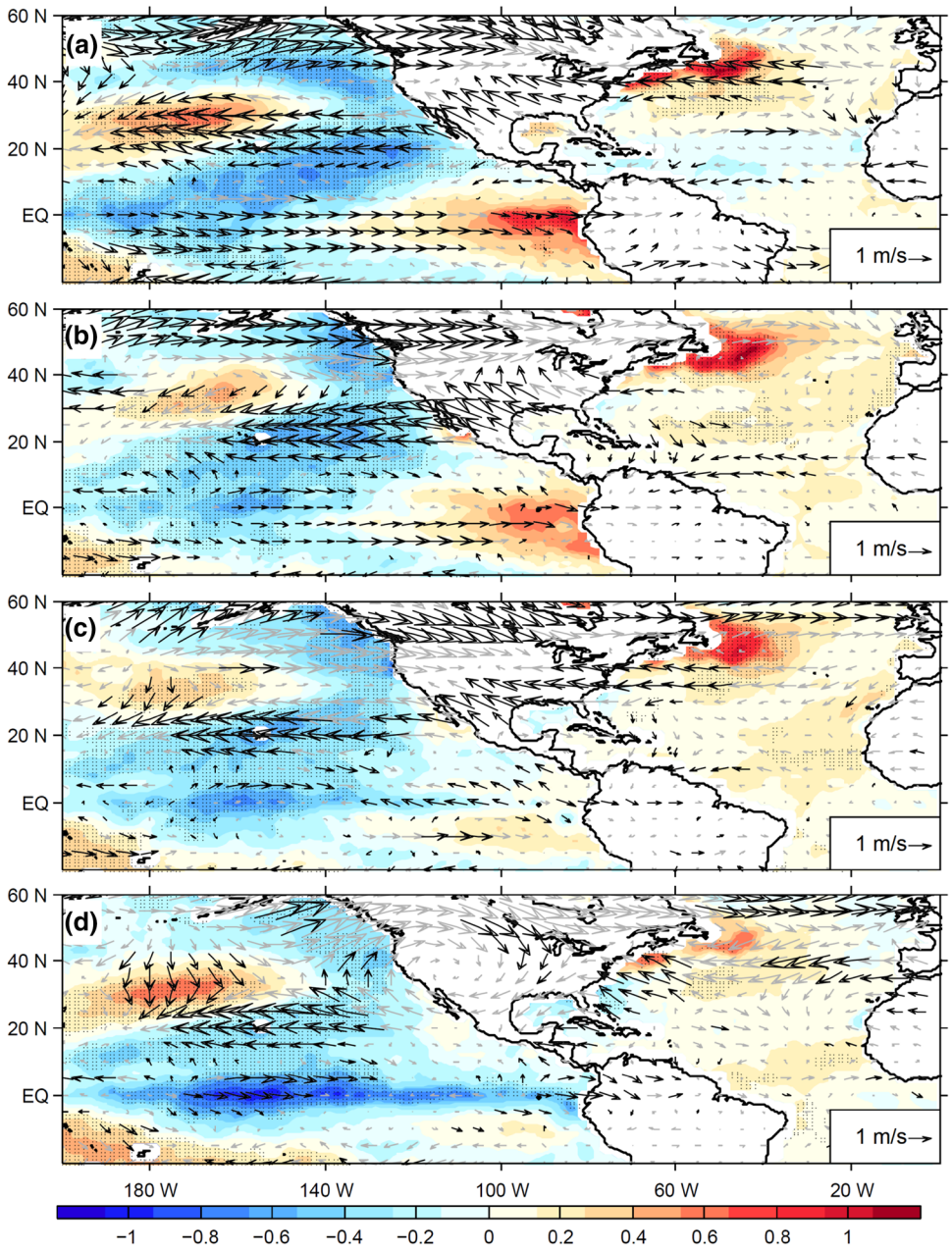

Fig. 10 Same as Fig. 9 but for the negative MAM PMM years

phase. This is also supported by the TC genesis anomalies during the positive and negative PMM phases. The time-lagged association between MAM PMM and ASO TC landfall is therefore largely attributed to the changes in both genesis and steering flow.

4.2 Modeling results using FLOR

To further verify the impacts of PMM on TC landfall over the US coast, we performed a set of perturbation experiments with GFDL FLOR, where SST is partially allowed to change. The SST anomalies associated with the positive PMM pattern propagated from the subtropical eastern Pacific to tropical central Pacific in ASO (Fig. 11). In ASO, the PPMM pattern (PPMM minus CTRL) produces the strongest SST warming in the tropical central Pacific (Fig. 11a) while the SST warming was originally the strongest in the subtropical eastern Pacific in PPMM (Fig. 11b). This suggests that the SST anomalies associated with PPMM tend to be followed by the central Pacific warming, which has been widely documented in the literature (e.g., Kim et al. 2012; Ding et al. 2015; Lin et al. 2015). Such tropical Pacific warming strongly modulates TC activity in the North Atlantic. Moreover, the TC density and genesis anomalies in PPMM minus CTRL experiments are strongly negative along the US coast and in the

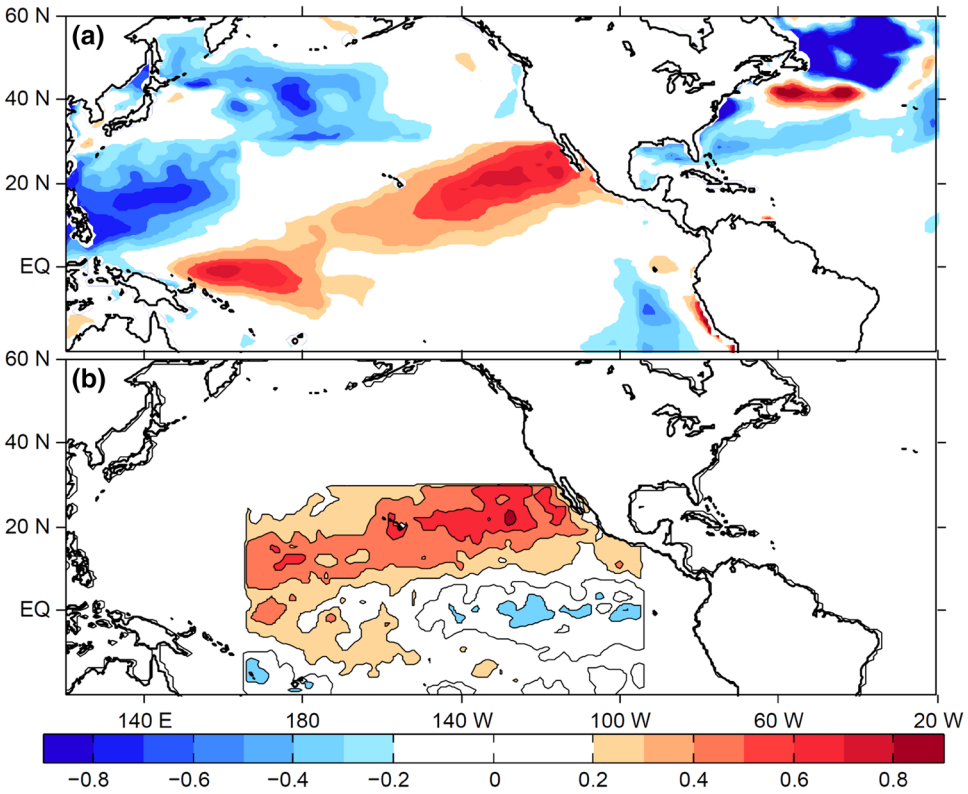

Fig. 11 **a** Simulated SST anomalies in (*shading* unit: °C) in PPMM minus CTRL experiments (ASO) and **b** the positive PMM pattern used in the PPMM experiment

North Atlantic (Fig. 12), suggesting a suppression of TC landfall during ASO with positive PPMM. The steering flow anomalies in PPMM minus CTRL experiments are characterized by westerly and they are comparable with those in the observations (Fig. 13). The westerly steering flow in PPMM minus CTRL experiments is consistent with less TC landfalls during the positive MAM PMM phase (Fig. 13). The steering flow anomalies are consistent with the anomalous 200 hPa geopotential height, which features a wave train propagating from the tropical Pacific to North America, similar to the PNA pattern. This suggests that the central Pacific warming may modulate TC landfall by triggering atmospheric teleconnections, which is also supported by previous findings showing that the central Pacific El Niño is strongly associated with the PNA pattern (e.g., Ashok et al. 2007; Weng et al. 2007, 2009). Similar to the observations, the differences in steering flow between FLOR experiments are not statistically significant along the US, Caribbean and Mexican coasts, though the differences in steering flow largely support the association between the landfalling TCs and PMM.

5 Conclusions

Improved understanding of the physical controls on North Atlantic TCs making landfall along the coast of the US, Caribbean Islands and Mexico has been the subject of large interest by the scientific community because of the catastrophic effects that these storms can have. Here we examined the role played by the PMM and its impact on North Atlantic landfalling TCs.

We found that there is a statistically significant time-lagged association between MAM PMM and the ASO TC landfall activity along the US coast (especially along the Gulf of Mexico and Florida) and Caribbean Islands. Specifically, the positive (negative) MAM PMM events tend to be followed by fewer (more) landfalling TCs over the US and Caribbean Islands in the following peak season. This lagged association is mainly caused by the lagged impacts of PMM on ENSO, and the subsequent impacts of ENSO on TC landfall. Positive (negative) PMM events are largely followed by El Niño (La Niña) events, which lead to less (more) TC geneses close to the US and Caribbean coastlines (i.e., the Gulf of Mexico and Caribbean Sea) and easterly (westerly) steering flow in the vicinity of the US and Caribbean coast: these conditions are in turn unfavorable (favorable) for TC landfalling across the Gulf of Mexico and Florida. Although concurrent (ASO) PMM has some impacts on the peak-season TC landfall activity, the impacts are weaker than the lagged impacts induced by MAM PMM.

The steering flow for TCs in the North Atlantic can be modulated by the Atlantic warm pool, the Atlantic Meridional Mode and ENSO (e.g., Kossin et al. 2010; Colbert and Soden 2012; Wang et al. 2011). Moreover, the steering flow

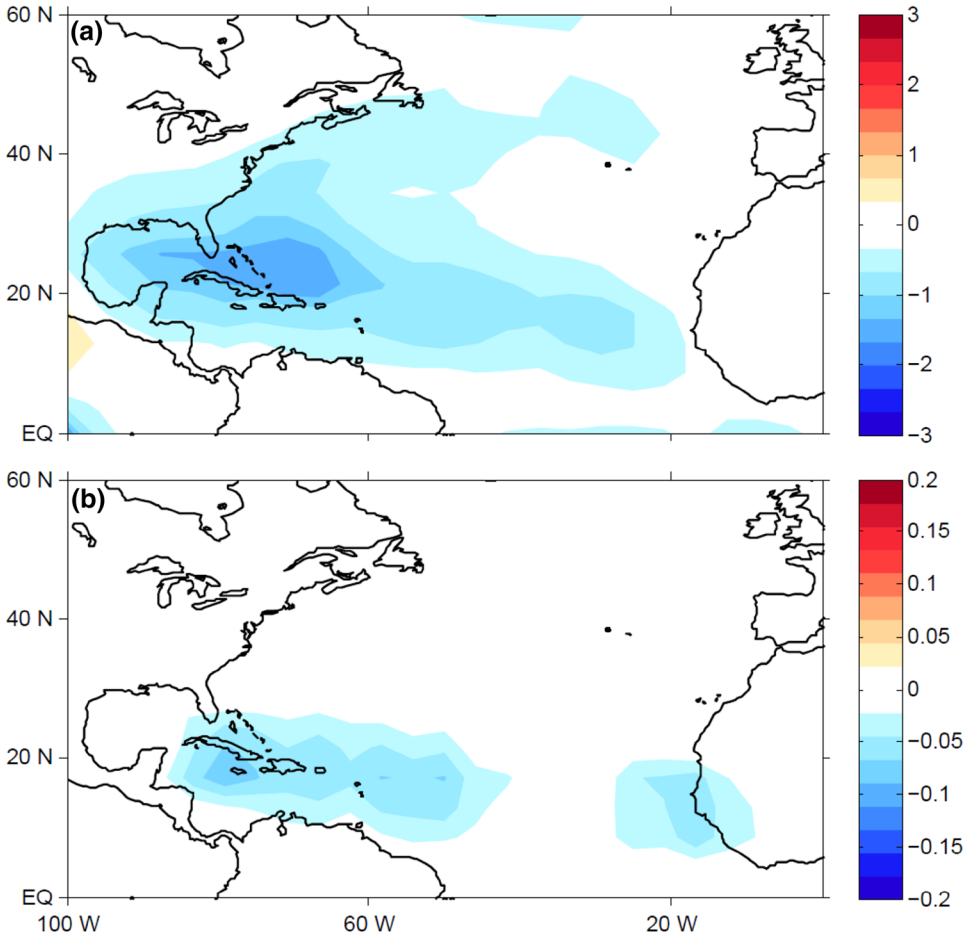

Fig. 12 Responses of North Atlantic TC **a** density (*shading* unit: occurrences/season) and **b** genesis (*shading* unit: occurrences/season) to the positive PMM (PPMM minus CTRL) in FLOR experiments

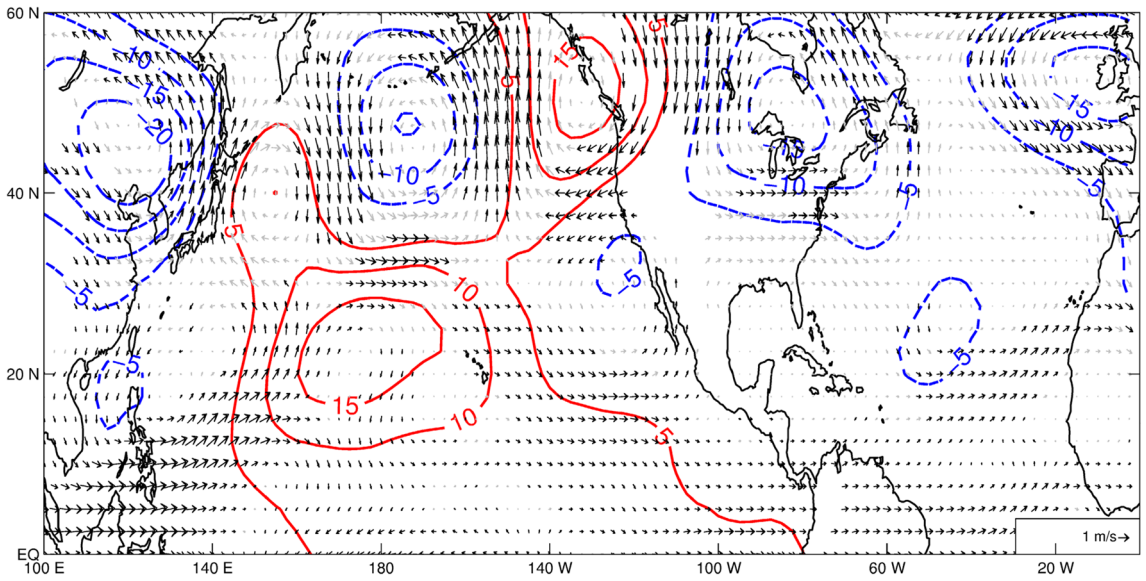

Fig. 13 Responses of steering flow (*vector* unit: ms^{-1}) and 200-hPa geopotential height (*contours* unit: gpm) to positive PMM (PPMM minus CTRL) in FLOR experiments. The *black wind vectors* are statistically significant at the 0.05 level

in the North Atlantic can also be modulated by the tropical Pacific SST forcing due to the Matsuno–Gill responses (Li et al. 2015). The PNA pattern may bridge the influences of the central Pacific El Niño on steering flow. The present study therefore provides insights into the impacts of the central Pacific warming on TC activity in the North Atlantic. Further analysis on the verification of such mechanisms underpinning changes in steering flow will be the focus of our future study.

Based on the analysis of the impacts of PMM on the North Atlantic landfalling TCs, the results also suggest that PMM should influence basinwide TC activity in the North Atlantic, shown in both observations and climate simulations with FLOR.

The time-lagged impacts of MAM PMM on TC landfall provide the scientific and operational community with a new quantity that can be potentially useful to forecast the seasonal frequency of landfalling North Atlantic TCs, especially over the Gulf of Mexico, Florida and Caribbean Islands. In addition, current seasonal prediction model for TC landfall may be improved if PMM can be satisfactorily predicted by current climate models in boreal spring.

Acknowledgements The authors are grateful to the reviewers for insightful comments. The authors acknowledge funding from the National Science Foundation under Grant No. AGS-1262099, and Award NA14OAR4830101 from the National Oceanic and Atmospheric Administration, US Department of Commerce.

References

Anderson BT (2003) Tropical Pacific sea-surface temperatures and preceding sea level pressure anomalies in the subtropical North Pacific. J Geophys Res 108:4732. doi:10.1029/2003JD003805

Anderson BT (2004) Investigation of a large-scale mode of ocean-atmosphere variability and its relation to tropical Pacific sea surface temperature anomalies. J Clim 17:4089–4098

Ashok K, Behera SK, Rao SA, Weng H, Yamagata T (2007) El Niño Modoki and its possible teleconnection. J Geophys Res 112:C11007

Boschat G, Terray P, Masson S (2013) Extratropical forcing of ENSO. Geophys Res Lett 40:1605–1611

Bove MC, O'Brien JJ, Eisner JB, Landsea CW, Niu X (1998) Effect of El Niño on US landfalling hurricanes, revisited. Bull Am Meteorol Soc 79:2477–2482

Camargo SJ, Robertson AW, Gaffney SJ, Smyth P, Ghil M (2007) Cluster analysis of typhoon tracks. Part II: large-scale circulation and ENSO. J Clim 20:3654–3676

Chan JCL, Gray WM (1982) Tropical cyclone movement and surrounding flow relationships. Mon Weather Rev 110:1354–1374

Chang P, Ji L, Li H (1997) A decadal climate variation in the tropical Atlantic Ocean from thermodynamic air-sea interactions. Nature 385:516–518

Chang P et al (2007) Pacific meridional mode and El Niño—southern oscillation. Geophys Res Lett 34:L16608

Chiang JC, Bitz CM (2005) Influence of high latitude ice cover on the marine intertropical convergence zone. Clim Dyn 25:477–496

Chiang JCH, Vimont DJ (2004) Analogous Pacific and Atlantic meridional modes of tropical atmosphere–ocean variability*. J Clim 17:4143–4158

Colbert AJ, Soden BJ (2012) Climatological variations in North Atlantic tropical cyclone tracks. J Clim 25:657–673

Delworth TL et al (2006) GFDL's CM2 global coupled climate models. Part I: formulation and simulation characteristics. J Clim 19:643–674

Delworth TL et al (2012) Simulated climate and climate change in the GFDL CM2.5 high-resolution coupled climate model. J Clim 25:2755–2781

Deser C, Wallace JM (1987) El Niño events and their relation to the southern oscillation: 1925–1986. J Geophys Res Oceans 92:14189–14196

Di Lorenzo E, Liguori G, Schneider N, Furtado J, Anderson B, Alexander M (2015) ENSO and meridional modes: a null hypothesis for Pacific climate variability. Geophys Res Lett 42:9440–9448

Ding R, Li J, Tseng YH, Sun C, Guo Y (2015) The Victoria mode in the North Pacific linking extratropical sea level pressure variations to ENSO. J Geophys Res Atmos 120:27–45

Elsner JB (2003) Tracking hurricanes. Bull Am Meteorol Soc 84:353–356

Elsner JB, Jagger TH (2006) Prediction models for annual US hurricane counts. J Clim 19:2935–2952

Emanuel KA, Nolan DS (2004) Tropical cyclone activity and the global climate system. Preprints, 26th Conference on Hurricanes and Tropical Meteorology, Miami, FL, Amer. Meteor. Soc. A

Gill AE (1980) Some simple solutions for heat-induced tropical circulation. Q J R Meteorol Soc 106:447–462

Kalnay E et al (1996) The NCEP/NCAR 40-year reanalysis project. Bull Am Meteorol Soc 77(3):437–471

Kim H-M, Webster PJ, Curry JA (2010) Modulation of North Pacific tropical cyclone activity by three phases of ENSO. J Clim 24:1839–1849

Kim ST, Yu J-Y, Kumar A, Wang H (2012) Examination of the two types of ENSO in the NCEP CFS model and its extratropical associations. Mon Weather Rev 140:1908–1923

Klotzbach PJ (2011) El Niño-southern oscillation's impact on Atlantic basin hurricanes and US landfalls. J Clim 24:1252–1263

Kossin JP, Camargo SJ, Sitkowski M (2010) Climate modulation of North Atlantic hurricane tracks. J Clim 23:3057–3076

Kug J-S, Jin F-F, An S-I (2009) Two types of El Niño events: cold tongue El Niño and warm pool El Niño. J Clim 22:1499–1515

Landsea CW, Franklin JL (2013) Atlantic Hurricane database uncertainty and presentation of a new database format. Mon Weather Rev 141:3576–3592

Larson SM, Kirtman BP (2014) The Pacific meridional mode as an ENSO precursor and predictor in the North American multimodel ensemble. J Clim 27:7018–7032

Larson S, Lee S-K, Wang C, Chung E-S, Enfield D (2012) Impacts of non-canonical El Niño patterns on Atlantic hurricane activity. Geophys Res Lett 39(14). doi:10.1029/2012GL052595

Lee S-K, Wang C, Enfield DB (2010) On the impact of central Pacific warming events on Atlantic tropical storm activity. Geophys Res Lett 37:L17702

Li W, Li L, Deng Y (2015) Impact of the Interdecadal Pacific Oscillation on Tropical Cyclone Activity in the North Atlantic and Eastern North Pacific. Sci Rep 5:12358. doi:10.1038/srep12358

Lin CY, Yu JY, Hsu HH (2015) CMIP5 model simulations of the Pacific meridional mode and its connection to the two types of ENSO. Int J Climatol 35:2352–2358

Marks FD, Shay LK (1998) Landfalling tropical cyclones: forecast problems and associated research opportunities. Bull Am Meteorol Soc 79:305–323

Matsuno T (1966) Quasi-geostrophic motions in the equatorial area. J Meteorol Soc Jpn 44:25–43
Murakami H et al (2016) Seasonal forecasts of major hurricanes and landfalling tropical cyclones using a high-resolution GFDL coupled climate model. J Clim 29:7977–7989
Murakami H et al (2017) Dominant role of subtropical pacific warming in extreme Eastern Pacific hurricane seasons: 2015 and the future. J Clim 30:243–264
Patricola CM, Saravanan R, Chang P (2014) The impact of the El Niño–southern oscillation and Atlantic meridional mode on seasonal Atlantic tropical cyclone activity. J Clim 27:5311–5328
Patricola CM, Chang P, Saravanan R (2016) Degree of simulated suppression of Atlantic tropical cyclones modulated by flavour of El Niño. Nat Geosci 9:155–160
Pegion K, Alexander M (2013) The seasonal footprinting mechanism in CFSv2: simulation and impact on ENSO prediction. Clim Dyn 41:1671–1683
Pielke R Jr, Landsea C (1999) La Niña, El Niño, and Atlantic hurricane damages in the US. Bull Am Meteorol Soc 80:2027–2033
Pielke R Jr, Gratz J, Landsea C, Collins D, Saunders M, Musulin R (2008) Normalized hurricane damage in the US: 1900–2005. Nat Hazards Rev 9:29
Rayner N et al (2003) Global analyses of sea surface temperature, sea ice, and night marine air temperature since the late nineteenth century. J Geophys Res 108:4407
Saunders MA, Lea AS (2005) Seasonal prediction of hurricane activity reaching the coast of the US. Nature 434:1005–1008
Smith AB, Katz RW (2013) US billion-dollar weather and climate disasters: data sources, trends, accuracy and biases. Nat Hazards 67:387–410
Smith SR, Brolley J, O'Brien JJ, Tartaglione CA (2007) ENSO's impact on regional US hurricane activity. J Clim 20:1404–1414
Staehling EM, Truchelut RE (2016) Diagnosing US hurricane landfall risk: an alternative to count-based methodologies. Geophys Res Lett 43:8798–8805
Tang BH, Neelin JD (2004) ENSO influence on Atlantic hurricanes via tropospheric warming. Geophys Res Lett 31:L24204
Vecchi GA, Villarini G (2014) Next season's hurricanes. Science 343:618–619
Vecchi GA et al (2014) On the seasonal forecasting of regional tropical cyclone activity. J Clim 27:7994–8016
Velden CS, Hayden CM, Paul Menzel W, Franklin JL, Lynch JS (1992) The impact of satellite-derived winds on numerical hurricane track forecasting. Weather Forecast 7:107–118
Villarini G, Vecchi GA, Smith JA (2011) US landfalling and North Atlantic hurricanes: statistical modeling of their frequencies and ratios. Mon Weather Rev 140:44–65
Vimont DJ, Kossin JP (2007) The Atlantic meridional mode and hurricane activity. Geophys Res Lett 34:L07709
Vimont DJ, Battisti DS, Hirst AC (2001) Footprinting: a seasonal connection between the tropics and mid-latitudes. Geophys Res Lett 28:3923–3926
Vimont DJ, Wallace JM, Battisti DS (2003) The seasonal footprinting mechanism in the Pacific: implications for ENSO*. J Clim 16:2668–2675
Walker GT, Bliss E (1932) World weather. V Mem R Meteorol Soc 4:53–84
Wang C, Lee S-K (2007) Atlantic warm pool, Caribbean low-level jet, and their potential impact on Atlantic hurricanes. Geophys Res Lett 34:L02703. doi:10.1029/2006GL028579
Wang C, Lee SK, Enfield DB (2008) Atlantic warm pool acting as a link between Atlantic multidecadal oscillation and Atlantic tropical cyclone activity. Geochem Geophys Geosyst 9:Q05V03. doi:10.1029/2007GC001809
Wang C, Liu H, Lee S-K, Atlas R (2011) Impact of the Atlantic warm pool on United States landfalling hurricanes. Geophys Res Lett 38:L1907. doi:10.1029/2011GL049265
Wang H et al (2014) How well do global climate models simulate the variability of Atlantic tropical cyclones associated with ENSO? J Clim 27:5673–5692
Weng H, Ashok K, Behera S, Rao S, Yamagata T (2007) Impacts of recent El Niño Modoki on dry/wet conditions in the Pacific rim during boreal summer. Clim Dyn 29:113–129
Weng H, Behera SK, Yamagata T (2009) Anomalous winter climate conditions in the Pacific rim during recent El Niño Modoki and El Niño events. Clim Dyn 32:663–674
Xie S-P, SGH Philander (1994) A coupled ocean-atmosphere model of relevance to the ITCZ in the eastern Pacific. Tellus A 46:340–350
Xie L, Yan T, Pietrafesa LJ, Morrison JM, Karl T (2005) Climatology and interannual variability of North Atlantic hurricane tracks. J Clim 18:5370–5381
Zhang L, Chang P, L Ji (2009a) Linking the Pacific meridional mode to ENSO: coupled model analysis. J Clim 22:3488–3505
Zhang L, Chang P, Tippett MK (2009b) Linking the Pacific meridional mode to ENSO: utilization of a noise filter. J Clim 22:905–922
Zhang W, Vecchi GA, Murakami H, Villarini G, Jia L (2016) The Pacific meridional mode and the occurrence of tropical cyclones in the western North Pacific. J Clim 29:381–398
Zhang W, Vecchi GA, Villarini G, Murakami H, Gudgel R, Yang X (2017) Statistical–dynamical seasonal forecast of western North Pacific and East Asia landfalling tropical cyclones using the GFDL FLOR coupled climate model. J Clim 30:2209–2232. doi:10.1175/JCLI-D-16-0487.1